Desalination and Water Treatment
www.deswater.com
2 (2009) 223–230
1944-3994/1944-3986

Mesoporous CeO_2-ZrO_2-γ-Al_2O_3 nanocomposite membranes exhibiting remarkable hydrothermal stability

Md. Hasan Zahir*, Shinji Fujisaki, Koji Sato, Takayuki Nagano, Yuji Iwamoto**

Japan Fine Ceramics Center, Hybrid Process Group, Nagoya 456-8587, Japan
Tel. +81 52 871 3500; Fax: +81 52 871 3599; email: hasan.zahir@gmail.com

Received 2 September 2007; Accepted 21 August 2008

ABSTRACT

The CeO_2-ZrO_2-γ-Al_2O_3 nanocomposite was synthesized through the sol-gel route by mixing a boehmite sol (AlOOH) with an appropriate amount of metal nitrates. By using this multicomponent sol, crack and pinhole free mesoporous membranes were successfully fabricated on an asymmetric porous α-Al_2O_3 support through dip coating process. The hydrothermal (up to 75% steam) stability of the mesoporous membranes was studied in terms of hydrogen gas permeance at 500°C, phase structure, surface microstructure and pore size distribution. The pore size distribution measurements were conducted directly on the membranes by a nano-permporometer. Among the tested samples with different molar compositions of CeO_2-ZrO_2-γ-Al_2O_3, only the mesoporous CeO_2-ZrO_2-γ-Al_2O_3 membrane with a molar ratio of 10:10:80 mol% was found to be the most effective membrane under the hydrothermal condition at 500°C. The ternary CeO_2-ZrO_2-γ-Al_2O_3 system retained its structure (order and porosity) after crystallization on an α-Al_2O_3 porous support and subsequent hydrothermal treatment for over 50 h. The hydrothermal test indicates that the mesoporous membrane developed in this study is viable to be used as an intermediate layer for fabricating a multilayer hydrogen separation membrane reactor for the methane steam reforming reaction.

Keywords: Mesoporous membrane; Ce-Zr solid solution; γ-Al_2O_3, Gas permeance; Hydrothermal stability

1. Introduction

It is important to develop an efficient hydrogen production method for a future energy system. Among various hydrogen sources, about 50% of world's hydrogen is produced from natural gas (CH_4, the main constituent of natural gas) and naphtha by means of steam-reforming reactions, which are thermodynamically well understood to favorably proceed at higher temperatures (>800°C) and lower pressures. If hydrogen (H_2) can be selectively removed from the reforming reactor through a H_2-permselective membrane, the thermodynamic equilibrium can be shifted to the product side, resulting in a higher conversion of CH_4 to H_2 even at lower temperatures (~500°C). Some researchers have already confirmed experimentally the phenomena by continuous removal of H_2 from the reaction system through inorganic membranes [1–3]. The important things in the membrane application to the reactors are the membrane characteristic permeance, selectivity and stability in steam at high temperatures.

A state-of-the-art microporous amorphous silica-based membrane is one candidate for developing a novel

*Corresponding author.
**Present address: Department of Materials Science and Engineering, Graduate School of Engineering, Nagoya Institute of Technology, Gokiso-cho, Showa-ku, Nagoya 466-8555, Japan.

membrane reactor. Generally, the microporous amorphous silica-based membrane can be fabricated on a porous support and, an important structural feature is an intermediate layer i.e., mesoporous (2 nm < ⌀ < 50 nm) γ-Al_2O_3 membrane, which is placed between the layer of a hydrogen perm-selective microporous amorphous silica-based membrane on the upper side and the surface of an α-Al_2O_3 porous support on the inner side [4]. The mean pore size of the mesoporous γ-Al_2O_3 intermediate layer is controlled to be about 4 nm. However, a small amount of larger macropores (⌀ >50 nm) sometimes exists in the intermediate layer, which leads to the formation of pinholes or cracks in the microporous amorphous silica-based membranes. To develop high-performance hydrogen separation membranes, it is important to develop technologies for fabricating a fine mesoporous intermediate layer as well as fabricating a molecular-sieve microporous membrane. Moreover, in the above-mentioned processes, high operation temperatures are necessary while the reaction atmospheres usually contain considerable amounts of steam because water is one of the reactants, or because steam is added to reduce coke formation. Thus, in many applications, the mesoporous intermediate layer (for example γ-Al_2O_3 membrane) must be sufficiently stable in environments of both increased temperature and containing steam. As humid atmospheres are more often encountered in industrial applications of these ceramic membranes, hydrothermal stability of the ceramic membranes is even more important from a practical viewpoint.

Addition of Al_2O_3 to the CeO_2-ZrO_2 (CZ) mixed oxides has been demonstrated to be a formidable tool that produces nanocomposite materials with high thermal stabilities [5]. Recently, it has been reported that the CZ system retains its structure (order and porosity) after crystallization on an α-Al_2O_3 support and subsequent thermal treatment to temperatures as high as 700°C [6]. Moreover, CZ-based mixed oxides are also current target of intensive research as a result of their applications in strategic technologies, such as the next generation of compact SOFC [7]. In view of these applications, controlling the porosity of these systems is highly desirable under both thermal as well as hydrothermal conditions. To date, relatively few papers have been devoted to this topic of extensive studies in this area. There are some reports on the CeO_2-ZrO_2-Al_2O_3 (CZA) system prepared by the sol-gel method using a templating agent [8,9], but the lack of information regarding the nature of characteristic properties of this system is a drawback, particularly regarding the microstructure, pore-size, and thermal as well as hydrothermal stability of the CZA system. Recently, we have systemically studied the textural and structural properties with different molar compositions of CZA nanocomposite powders under hydrothermal conditions [10,11]. The choices of the appropriate CZ precursor and addition to boehmite sol were found to be very critical factors to obtain a hydrothermally stable porous structure system under mild intermediate temperatures as 500°C. However, we have been able to optimize a highly hydrothermally stable CZA nano-composite powder system. The favorable stability of the CZA system in both structural and textural properties gives promise of the application of a membrane reactor as an intermediate layer (membrane) to meet the increasingly stringent requirement of service life of a top separation amorphous silica-based layer under hydrothermal conditions.

In order to examine the hydrothermal (up to 75%) stability of the mesoporous CZA nanocomposite membranes at 500°C, the mesoporous membranes with different molar composition were fabricated on an α-Al_2O_3 porous support. The stability was studied in terms of the phase structure and surface microstructure before and after the hydrothermal treatment, as well as the H_2 gas permeance performance in steam at 500°C. The pore structure evolution during the hydrothermal treatment was also studied directly on the membranes by nano-permporometer.

2. Materials and experimental procedures

2.1. Synthesis

Mesoporous nanocomposite membranes based on CeO_2-ZrO_2-Al_2O_3 materials was synthesized by the sol-gel method, and hereafter, they are referred to as XX**C** YY**Z** ZZ**A**, where XX, YY and ZZ indicate the molar percentages of CeO_2, ZrO_2 and Al_2O_3, respectively (for example, 10C10Z80A), as shown in Table 1. Sols were prepared by reacting 0.5 mole of aluminium-tri-sec-butoxide (Al(O-s-Bu)$_3$ = ATSB, 97%, Aldrich, USA) with double-distilled water at 90°C. After the addition of ATSB, the mixture was maintained at 90°C for at least 1 h to evaporate off the butanol that formed. The mixture was subsequently cooled to approximately at 60°C and peptized with 1 M HNO_3 at a pH of about 3. During the synthesis, the sol was stirred vigorously. The peptized mixture was refluxed at 90°C for 12 h, yielding a very stable 0.5 molar boehmite sol with a clear whitish-blue appearance. Doping of this sol was performed by mixing it with an aqueous solution of $Ce(NO_3)_3 \cdot 6H_2O$ (Kanto Kagaku, Japan) and/or $ZrO(NO_3)_2 \cdot 2H_2O$ (Wako Pure Chemical, Japan). The compositions [metal nitrate (mol%): boehmite (mol%)] of various precursor solutions for sol synthesis are shown in Table 1. For example, the amount of $Ce(NO_3)_3 \cdot 6H_2O$ corresponding to the added 5 to 35 mol% CeO_2 was calculated as

$$[\text{mol Ce}/(\text{mol Ce} + \text{mol ATSB})] \times 100\% \quad (1)$$

Table 1
Tested samples prepared by the sol-gel method and their compositions in mol%

Sample	Composition (mol%)	Abbreviation
γ-Al_2O_3	100	γAl_2O_3
CeO_2-ZrO_2-Al_2O_3	5:5:90	5C5Z90A
CeO_2-ZrO_2-Al_2O_3	10:10:80	10C10Z80A
CeO_2-ZrO_2-Al_2O_3	20:20:60	20C20Z60A
CeO_2-ZrO_2-Al_2O_3	35:35:30	35C35Z30A

The increase in the sol viscosity upon the addition of the nitrate solution was probably a result of a decrease in the pH due to the acidity of the nitrate solution. The doped boehmite sols were therefore prepared without the addition of HNO_3.

2.2. Membrane preparation

A dip-coating solution was obtained by diluting boehmite sol (γ-AlOOH) with a 3.5 wt% solution of polyvinyl alcohol (PVA, Kanto Chemical, Japan; MW = 72,000) prepared by refluxing at 90°C for 3 h. It has been reported that the pore-size distributions of γ-Al_2O_3 membranes with the addition of PVA do not show a measurably altered pore structure [12]. Unless stated otherwise, all γ-Al_2O_3-based nanocomposite membranes in this paper were prepared by adding PVA to the boehmite colloidal suspension.

The porous support used in the present study was an α-Al_2O_3 (ϕ 6 mm, L 80 mm, porosity 43%, and mean pore diameter of inner side and outer surface were 1.1 mm and 80 nm, respectively: Noritake, Japan). Before the dip-coating step, the graded α-Al_2O_3 support was cleaned by rinsing in acetone. The dried porous support was brought into contact with the boehmite sol. After a certain period (on the order of seconds), the support was removed and the gel layer was dried and all the dried samples were calcined from ambient temperature to 600°C at a heating rate of 1ºC/min and then maintained at 600°C for 3 h, followed by gradual cooling (2°C/min) to room temperature. The whole process of dipping, drying, and calcining was repeated once to repair any defects in the first γ-Al_2O_3-based nanocomposite layer. These samples are indicated as the "as-prepared" membranes.

2.3. Hydrothermal treatment

In order to understand the hydrothermal stability of the CZA systems investigated in this study, the powdered samples were exposed to steam using a Teflon-lined stainless-steel autoclave, maintaining the feed molar ratio of N_2:H_2O at 1:3 at 500°C.

In the case of the mesoporous CeO_2-ZrO_2-γ-Al_2O_3 nanocomposite membranes, the H_2 gas permeability was measured at 500°C, maintaining the feed molar ratio of N_2:H_2O (steam) at 1:3. These N_2/steam streams were fed to the heated module. The steam was condensed and collected from both the reject and permeates streams. Before the permeances were measured, the water flow was halted at the specified time intervals. The gas permeance performance was evaluated by the volumetric method at constant pressure [13]. More than five measurements were made and the average value was recorded.

2.4. Characterization

X-ray diffraction (XRD) patterns were recorded using an X-ray diffractometer (Rigaku, RINT-2000) with a Cu Kα radiation of 50 keV and 200 mA with a monochromator over a diffraction angle range 2q from 10 to 80° at a scan rate of 2°/min by analyzing the respective powdered samples prepared by calcining the original boehmite sols. The morphology and thickness of the membranes were examined by scanning electron microscopy (SEM; Hitachi S-4500, Tokyo, Japan, operated at 20 keV). The pore-size distribution measurements were conducted directly on the membrane by nano-permporometer (Seika, Japan) [13–15].

3. Results and discussion

3.1. H_2 gas permeance performance after hydrothermal treatment

The typical thicknesses of some selected membranes were observed to be in the range of 3–3.5 μm from the cross-sectional SEM images of the membranes, as shown in Fig. 1. The effect of the 500°C hydrothermal treatment with a 75% steam stream on the H_2 gas permeance through the mesoporous membranes is shown in Fig. 2. The 0 h in Fig. 2 represents the H_2 gas permeance at 500°C without the presence of steam. After the first measurement at 0 h, the remainder of the permeance data was obtained under the hydrothermal condition. The H_2 gas permeance of γ-Al_2O_3 membrane drastically increased, i.e., from 7.50 to 9.37×10^{-6} (mol m^{-2} s^{-1} Pa^{-1}) within the first 2 h in steam. Then the H_2 gas permeance increased steeply with increase in exposure time in the presence of steam. Gallaher et al. [16] investigated the hydrothermal (up to 90% steam) stability of commercial γ-Al_2O_3 membranes by H_2 gas permeation. They found that the H_2 gas permeances increased rapidly, as a function of hydrothermal treatment duration. The results indicate that the mesoporous γ-Al_2O_3 membrane is not a good candidate for use as an intermediate layer for the fabrication of microporous

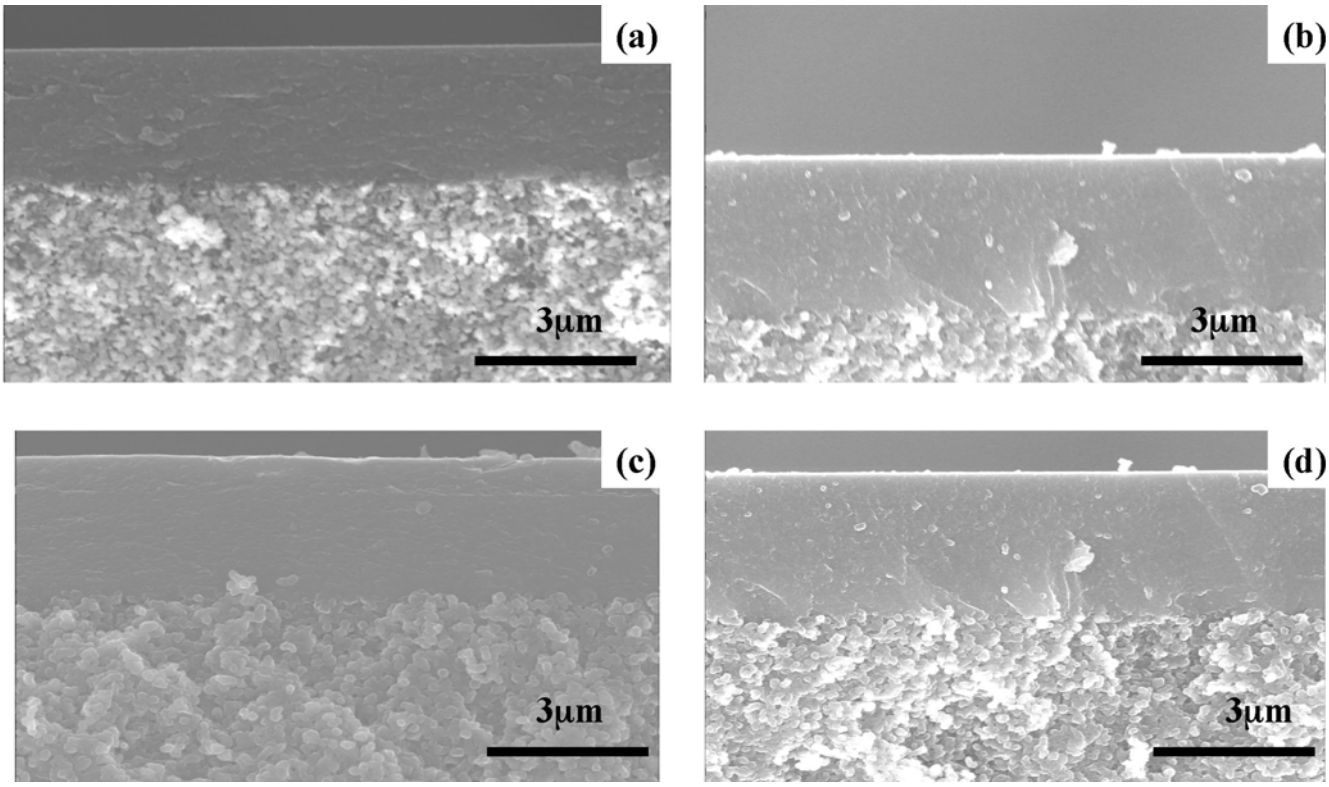

Fig. 1. SEM cross sectional images of (a) γ-Al_2O_3, (b) 5C5Z90A, (c) 10C10Z80A, and (d) 20C20Z60A membranes on an α-Al_2O_3 porous support.

gas separation membranes. The mesoporous intermediate layer must be stable under hydrothermal conditions to minimize the formation of defects in the microporous top layer. Like γ-Al_2O_3, at lower content of CZ into γ-Al_2O_3 i.e., 5C5Z90A system also showed a rapid initial increase in the H_2 permeance and the subsequent H_2 permeance increased very slowly after that as shown in Fig. 2. The 10C10Z80A membrane with molar ratio of 10:10:80 (Ce:Zr:Al), showed a little increase (ca. 2%) of H_2 gas permeance at the initial stage, and the subsequent permeance maintained almost a constant value during the hydrothermal test. This result is reminiscent of our recent findings that an intermediate molar ratio of CZ into γ-Al_2O_3 nanocrystalline oxide powders maintained a stable pore size distribution in mesopore range before and after the hydrothermal treatment at 500°C [10,11]. In the case of 20C20Z60A, the H_2 permeance remarkably increased from 7.55 to 8.75×10^{-6} (mol m^{-2} s^{-1} Pa^{-1}) within the first 2 h in steam. At higher content of CZ, i.e., of 35C35Z30A sample, a very large difference was observed between the 10C10Z80A and 35C35Z30A samples within the first 2 h of the hydrothermal test. The results revealed that a large amount of CZ (at and above 40 mol%) into the γ-Al_2O_3 system was not advantageous for fabricating a hydrothermally stable intermediate layer.

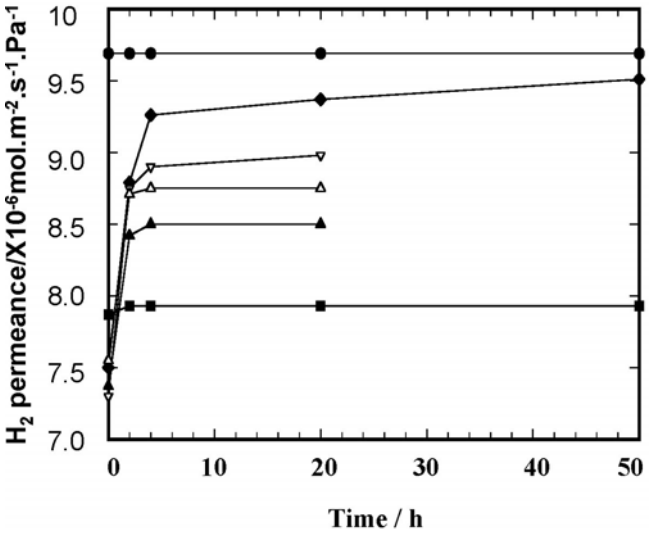

Fig. 2. Effect of steam on the time course of H_2 gas permeance for an α-Al_2O_3 porous support alone (●), mesoporous γ-Al_2O_3 (◆), 35C35Z30A (▽), 20C20Z60A (Δ), 10C10Z80A (■), and 5C5Z90A (▲) membranes at 500°C for 20 h. The H_2 gas permeance performance of γ-Al_2O_3 and 10C10Z80A membranes for 50 h has been performed and inserted. (The 0 h represents the H_2 permeance at 500°C without the presence of steam).

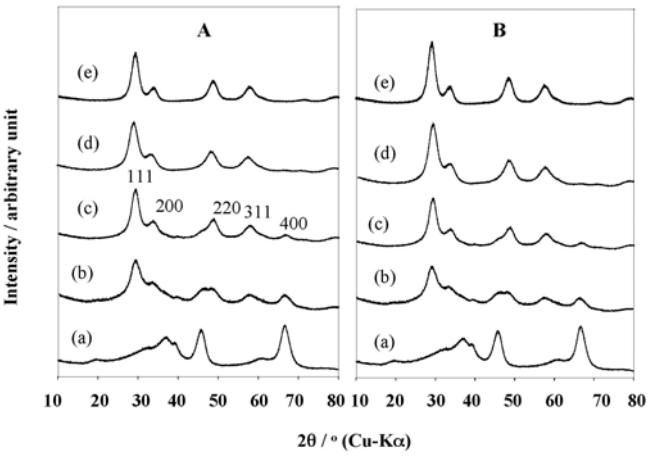

Fig. 3. X-ray diffraction patterns of powder (a) γ-Al_2O_3, (b) 5C5Z90A, (c) 10C10Z80A, (d) 20C20Z60A, (e) 35C35Z30A samples before (A) and after (B) hydrothermal treatment at 500°C for 4 h containing 75% steam.

3.2. Crystalline framework

The XRD patterns of all the powdered samples before and after the hydrothermal treatment are shown in Fig. 3. After the hydrothermal treatment at 500ºC, a slight increase in the peak intensity is observed in the XRD pattern of γ-Al_2O_3, indicating an increased crystallinity of γ-Al_2O_3 [Figs. 3(a)]. A mixed oxide phases of γ-Al_2O_3 and CeO_2-ZrO_2 solid solution was observed upon the addition of CeO_2 as well as ZrO_2 with a molar ratio of 5:5% added to γ-Al_2O_3, then the peak intensities of the two phases were almost unchanged after the hydrothermal treatment [Fig. 3(b)].

As previously studied and shown in Figs. 3(c)–(e), by increasing the amount of CZ added to γ-Al_2O_3, the crystallinity of the γ-Al_2O_3 matrix was remarkably decreased to be observed as X-ray amorphous, and the diffraction peaks due to the CeO_2-ZrO_2 solid solution appeared [11]. After the hydrothermal treatment, the peak intensity of the solid solution in the 10C10Z80A sample was almost unchanged [Fig. 3(c)], while those of the 20C20Z60A and 35C35Z30A samples exhibited an apparent increase in the crystallinity of the solid solution as evidenced by the strong peak, indexed as (111) plane, at about 29° (2q) [5] [Figs. 3(d) and (e)].

The chemical composition of the solid solution in the 10C10Z80A sample was estimated to be $Zr_{0.32}Ce_{0.68}O_2$ [10,11]. This result implies that, part of the Zr is not detected by the diffraction techniques and must be in a nearly amorphous form, as also occurs in CeO_2-ZrO_2-Al_2O_3 specimens prepared by coimpregnation [5]. Upon increasing the amount of CZ added to γ-Al_2O_3, i.e., 35C35Z30A sample, the chemical composition of the solid solution was estimated to be $Zr_{0.46}Ce_{0.54}O_2$, which was in agreement with the nominal composition of $Zr_{0.5}Ce_{0.5}O_2$ [10,11]. It has been reported that $Zr_{0.2}Ce_{0.8}O_2$ could be the most texturally stable $Ce_xZr_{1-x}O_2$ composition [17], whereas ZrO_2-rich compositions were found to be more thermally stable compared with CeO_2-rich ones in other studies [18]. In any case, it is known that considerably different textural and chemical behaviors can be achieved by changing the synthesis method of this system [17]. ZrO_2 segregation is a common feature in the CZA system [5,8,9]. Such ZrO_2 particle formation must occur inside the spinel channels of γ-Al_2O_3. The size of these ZrO_2 particles is too large to be accommodated by mere crystal expansion. We can only conclude that the spinel structure is damaged around these ZrO_2 particles. However, the damage remains sparse in the case of the 10C10Z80A system for the total loading of ZrO_2 (9 wt.%) used here. On the basis of the above discussion, we can say that the 10:10:80 system might be capable of maintaining a balance and/or appropriate chemical composition as well as retaining the rigid mesopore structure, particularly under hydrothermal conditions.

3.3. Microstructure

The typical differences in the surface morphology change of the selected membranes before and after the hydrothermal treatment are shown in Fig. 4. Very smooth morphology was observed for both as-prepared γ-Al_2O_3 and 10C10Z80A samples, as shown in Figs.4 (a) and (c). The surface of the steam-exposed 10C10Z80A membrane [Fig. 4(d)] was smooth and crack-free, whereas morphology with spherical grains was found on the γ-Al_2O_3 membrane [Fig. 4(b)]. The observed gas permeance was consistent with the morphological changes in the case of the γ-Al_2O_3 sample after the hydrothermal treatment.

3.4. Mesopore structure

In Fig. 5 the N_2 permeations are plotted as a function of the Kelvin diameter for γ-Al_2O_3 [Fig. 5 (a)] and 10C10Z80A [Fig. 5 (b)] samples. We have compared the 10C10Z80A sample with γ-Al_2O_3 in Fig. 5 because, as shown in Fig. 2, the 10C10Z80A membrane was found to be able to withstand at 500°C under hydrothermal conditions. When as-prepared γ-Al_2O_3 is used, lower values of the Kelvin diameter are found as shown in Fig. 5(a), open circle. However, the permeations of γ-Al_2O_3 obtained by the permporometer measurement were shifted to larger Kelvin diameters [Fig. 5(a), symbol (● and ■)] after the hydrothermal treatment for 4 and 50 h, respectively. The permeation change was negligible at higher Kelvin diameters in the case of the as-prepared 10C10Z80A membrane and after hydrothermal treatment. These results, in particular the short tail of the N_2 permeation

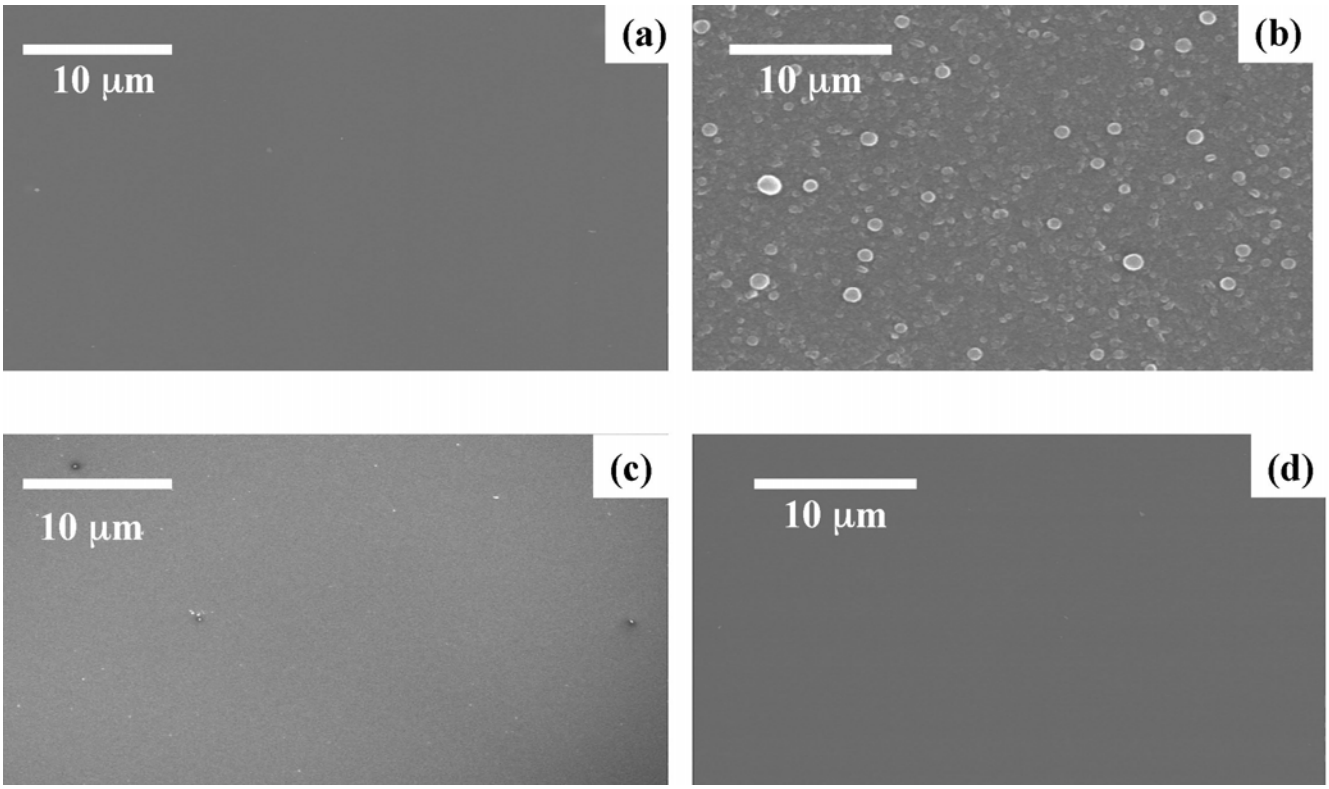

Fig. 4. SEM images of top surface view of (a) γ-Al_2O_3 and(c) 10C10Z80A membranes before and (b) γ-Al_2O_3 and (d) 10C10Z80A after hydrothermal treatment.

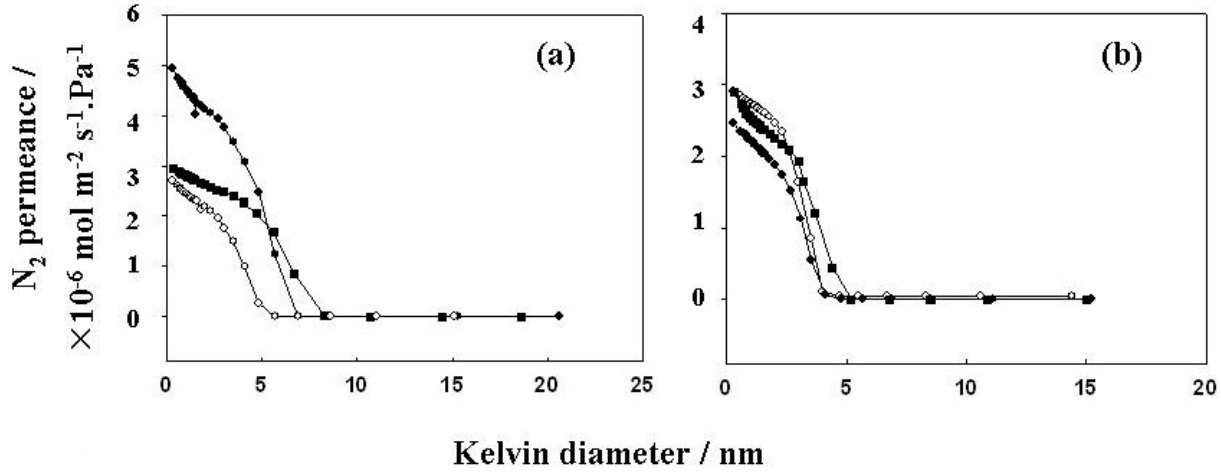

Fig. 5. N_2 permeance (measured by nano-permporometer) as a function of Kelvin diameter of (a) γ-Al_2O_3, and (b) 10C10Z80A, membranes before (○) and after (●) hydrothermal treatment for 4 h. The symbol (■) represents after hydrothermal treatment for 50 h.

after 50 h hydrothermal treatment, could be an indication of no larger pores existing in the specimen at higher Kelvin diameters [Fig. 5(b), symbol (■)], meaning that the 10C10Z80A mesoporous intermediate membrane is defect-free. Moreover, it revealed that there was no large number of pinholes before the hydrothermal stability test or large number pinholes were generated by the hydrothermal treatment.

The N_2 permeations and the calculated pore size distributions (PSDs) obtained by permporometry for the mesoporous membranes investigated in this study are also summarized and shown in Fig. 6. The calculated

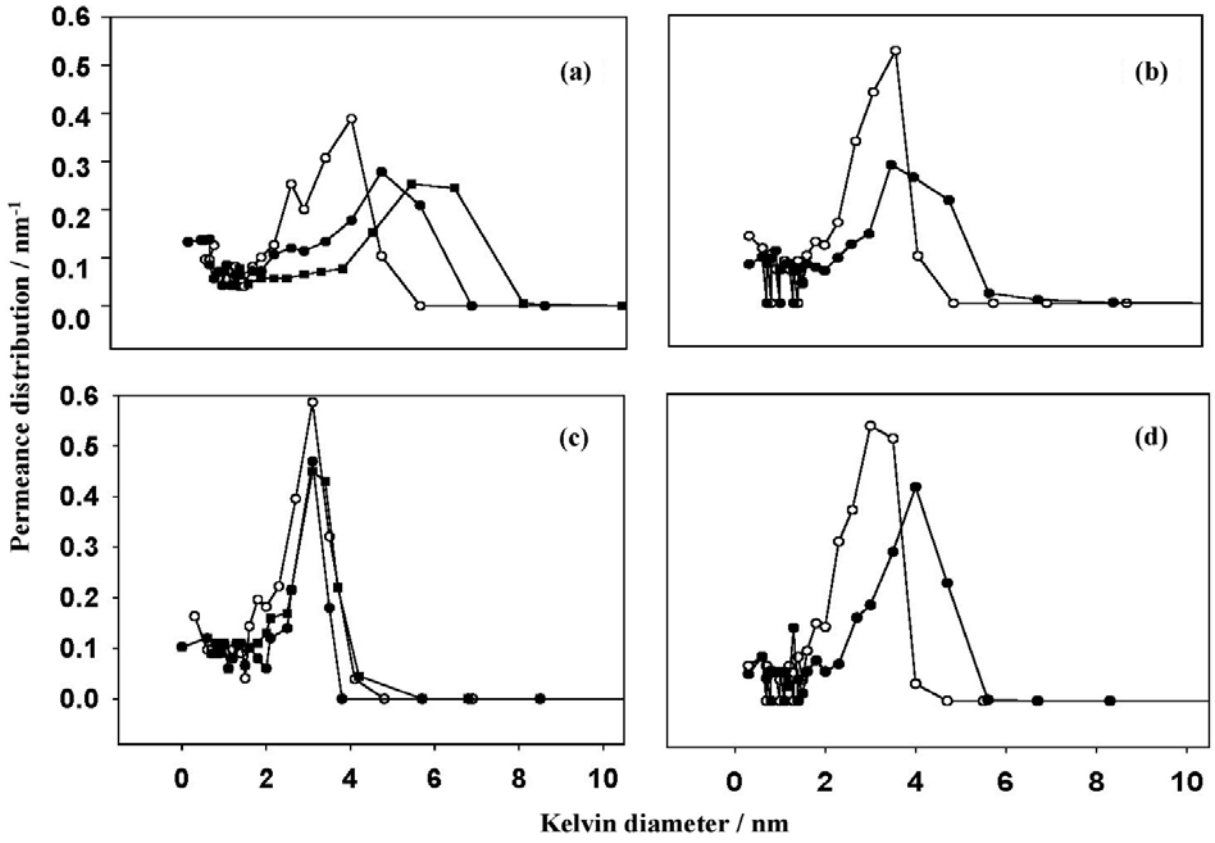

Fig. 6. Pore size distribution measured by nano-permporometer of (a) γ-Al_2O_3, (b) 5C5Z90A, (c) 10C10Z80A, and (d) 20C20Z60A membranes. Symbol as in Fig. 5.

PSDs show the distribution of the total number of pores within a certain range. The as-prepared γ-Al_2O_3 membrane [Fig.6(a), open circle] revealed that the permeation at large Kelvin radii was almost zero, and showed a strongly increased permeation at around 4–4.5 nm. This implies that no pores or only a few pores were present with Kelvin radii larger than 4.5 nm. The calculated maxima was found at r_k = 4.0 nm.

Compared with the as-prepared γ-Al_2O_3 membrane, the as-prepared CZA membranes exhibited a slight narrow pore size distribution located between 2.0–4.0 nm [Figs. 6(b)–(d), open circles]. However, after the prolonged steam exposure at 500°C for 20 h, the PSD of the 5C5Z90A and 20C20Z60A as well as the γ-Al_2O_3 membranes shifted toward larger pore diameter [Figs. 6 (a), (c) and (d), solid circles]. In contrast to these results, the PSD of the 10C10Z80A membrane was found to be almost unchanged even after the 20 h steam exposure at 500°C [Fig. 6(c), solid circles].

From the above permeability results, it is clear that the H_2 permeance of the sample membranes shown in Fig. 2 increases due to the increase in pore size as steam exposure time increases. In the case of mesoporous γ-Al_2O_3 membrane, the mean pore size continuously increased and the pore size distribution broadened during the 500°C-prolonged steam exposure for 50 h [Fig. 6(a), symbol (■)]. These results agree very well with those of Gallaher et al. [16].

Based on the results shown above, a subsequent study on the durability of the mesoporous 10C10Z80A membrane was performed. As a result, the 10C10Z80A membrane was found to be able to withstand for more than 50 h with no sign of degradation [Fig. 2 and Fig. 6(c), symbol (■)].

The resulting mesoporous inorganic frameworks of the 10C10Z80A membrane, prepared by a very convenient one-pot sol-gel method, are very promising. Usually, most of the previous studies were formed by preparing CZ solid solution and γ-Al_2O_3 and/or d-Al_2O_3 separately and then mixing the two powders [17,19]. Therefore, the particle distribution as well as the mesoporous structure development should be different from those in earlier studies. The high hydrothermal stability of the 10C10Z80A clearly points out a stabilization of the mesopore structure, which is due to the appropriate amount of the CeO_2-ZrO_2 rigid structure with interconnection by γ-Al_2O_3.

4. Conclusions

The present work reports the first example of a CeO_2-ZrO_2-γ-Al_2O_3 nanocomposite oxides system, which has the ability to produce crack- and pinhole-free mesoporous membranes on an α-Al_2O_3 porous support. The permeability and characterization results showed that the hydrothermal stability of the CeO_2-ZrO_2-γ-Al_2O_3 mesoporous membrane with a molar ratio of 10:10:80 was greatly improved in comparison with mesoporous γ-Al_2O_3. A very sharp pore size distribution curve was maintained for more than 50 h at a hydrothermal condition of 500°C. The unchanged H_2 gas permeance as well as phase structure revealed that the fabricated mesoporous membrane possessed extraordinarily high hydrothermal stability for a very long service period.

Acknowledgements

This work was carried out as a part of the R&D Project on Highly Efficient Ceramic Membranes for High-Temperature Separation of Hydrogen, supported by the New Energy and Industrial Technology Development Organization (NEDO), Japan.

References

[1] M. Chai, M. Machida, K. Eguchi and H. Arai, Promotion of hydrogen permeation on metal-dispersed alumina membranes and its application to a membrane reactor for methane reforming, Appl. Catal. A: Gen., 110 (1994) 239–250.
[2] T.T. Tsotsis, A.M. Champagnie, S.P. Vasileiadis, Z.D. Ziaka and R.G. Minet, The enhancement of reaction yield through the use of high temperature membrane reactors, Sep. Sci. Technol., 28 (1993) 397–402.
[3] E. Kikuchi, Membrane reactor application to hydrogen production, Catal. Today, 56 (2000) 97–101.
[4] R.M. De Vos and H. Verweij, High-selectivity, high-flux silica membranes for gas separation, Science, 279 (1998) 1710–1711.
[5] J. Kašpar and P. Fornasiero, Nanostructured materials for advanced automotive de-pollution catalysts, J. Solid State Chem., 171 (2003) 19–29.
[6] E.L. Crepaldi, G.J. de A.A. Soler-Illia, A. Bouchara, D. Grosso, D. Durand and C. Sanchez, Controlled formation of highly ordered cubic and hexagonal mesoporous nanocrystalline yttria-zirconia and ceria-zirconia thin films exhibiting high thermal stability, Angew. Chem. Int. Ed. Engl., 42 (2003) 347–351.
[7] B.C.H. Steele, Fuel-cell technology, running on natural gas, Nature, 400 (1999) 619–621.
[8] A.I. Kozlov, D.H. Kim, A. Yezerets, P. Andersen, H.H. Kung and M.C. Kung, Effect of preparation method and redox treatment on the reducibility and structure of supported ceria-zirconia mixed oxide, J. Catal., 209 (2002) 417–426.
[9] M.H. Yao, R.J. Baird, F.W. Kunz and T.E. Hoost, An XRD and TEM investigation of the structure of alumina-supported ceria-zirconia, J. Catal., 166 (1997) 67–74.
[10] Md.H. Zahir, T. Nagano and Y. Iwamoto, Ceria-zirconia-γ-alumina nanocomposite mesoporous membrane, Japanese Patent 171895, 2006.
[11] Md.H. Zahir, Y.H. Ikuhara, S. Fujisaki, K. Sato, T. Nagano and Y. Iwamoto, Preparation and characterization of mesoporous ceria-zirconia-alumina nanocomposite with high hydrothermal stability, J. Mater. Res., 22 (2007) 3201–3209.
[12] R.S.A. de Lange, J.H.A. Hekkink, K. Keizer and A.J. Burggraaf, Formation and characterization of supported microporous ceramic membranes prepared by sol-gel modification techniques, J. Membr. Sci., 99 (1995) 57–75.
[13] Md.H. Zahir, K. Sato, H. Mori, Y. Iwamoto, M. Nomura and S. Nakao, Preparation and properties of hydrothermally stable γ-alumina-based composite mesoporous membranes, J. Am. Ceram. Soc., 89 (2006) 2874–2880.
[14] T. Tsuru, T. Hino, T. Yoshioka and M. Asaeda, Permporometry characterization of microporous ceramic membranes, J. Membr. Sci., 186 (2001) 257–265.
[15] Md.H. Zahir, K. Sato and Y. Iwamoto, Development of hydrothermally stable sol-gel derived La_2O_3-doped Ga_2O_3-Al_2O_3 composite mesoporous membrane, J. Membr. Sci., 247 (2005) 95–101.
[16] G.R. Gallaher and P.K.T. Liu, Characterization of ceramic membranes 1. Thermal and hydrothermal stabilities of commercial 40 Å membranes, J. Membr. Sci., 92 (1994) 29–44.
[17] R. Di Monte and J. Kašpar, Heterogeneous environmental catalysis—a gentle art: CeO_2-ZrO_2 mixed oxides as a case history, Catal. Today, 100 (2005) 27–35.
[18] J. Cuif, G. Blanchard, O. Touret, A. Seigneurin, M. Marczi and E. Quémeré: (Ce,Zr)O_2 solid solutions for three-way catalysts, SAE Tech. Pap. Ser., 970463, 1997.
[19] J. Kašpar, P. Fornasiero and M. Graziani, Use of CeO_2-based oxides in the three-way catalysis, Catal. Today, 50 (1999) 285–298.